Computers and Mathematics with Applications 64 (2012) 2049–2065

Contents lists available at SciVerse ScienceDirect

Computers and Mathematics with Applications

journal homepage: www.elsevier.com/locate/camwa

A numerical solution of the nonlinear controlled Duffing oscillator by radial basis functions☆

J.A. Rad [a,*], S. Kazem [b], K. Parand [a]

[a] Department of Computer Sciences, Faculty of Mathematical Sciences, Shahid Beheshti University, Evin, Tehran 19839, Iran

[b] Department of Mathematics, Imam Khomeini International University, Ghazvin 34149-16818, Iran

ARTICLE INFO

Article history:
Received 24 June 2011
Received in revised form 3 December 2011
Accepted 28 March 2012

Keywords:
Optimal control problem
Duffing oscillator
Radial basis functions
Collocation method
Gaussian RBF
Lagrange multipliers

ABSTRACT

In this research, a new numerical method is applied to investigate the nonlinear controlled Duffing oscillator. This method is based on the radial basis functions (RBFs) to approximate the solution of the optimal control problem by using the collocation method. We apply Legendre–Gauss–Lobatto points for RBFs center nodes in order to use the numerical integration method more easily; then the method of Lagrange multipliers is used to obtain the optimum of the problems. For this purpose different applications of RBFs are used. The differential and integral expressions which arise in the dynamic systems, the performance index and the boundary conditions are converted into some algebraic equations which can be solved for the unknown coefficients. Illustrative examples are included to demonstrate the validity and applicability of the technique.

1. Introduction

1.1. Introduction of the problem

Optimal control problems arise in a wide variety of disciplines. Apart from traditional areas such as aerospace engineering, robotics and chemical engineering, the optimal control theory has also been used with great success in areas as diverse as economics to biomedicine and other areas of science and has received considerable attention of researchers.

Highly accurate solutions are needed to resolve the optimal control vector in the numerical solution of optimal control problems involving nonlinear dynamical systems. However, serious analytical and numerical difficulties, such as the accumulation of roundoff truncation errors, need to be overcome before optimal control approaches find widespread practical implementation, especially for nonlinear optimal control problems.

In recent years there has been much interest in the use of spectral methods for the solution of nonlinear physical and engineering problems. The main thrust of spectral methods has been inhibited due to their lack of application to controlled nonlinear dynamical systems. The controlled nonlinear Duffing oscillator is known to describe many important oscillating phenomena in some nonlinear physical and engineering systems [1–3]

$$J = \frac{1}{2}\int_{-T}^{0} U^2(\tau)d\tau, \tag{1}$$

☆ The paper has been evaluated according to old Aims and Scope of the journal.

* Corresponding author. Tel.: +98 937 509 2738; fax: +98 21 22431650.
E-mail addresses: ja.amani66@gmail.com, j.amanirad@gmail.com (J.A. Rad), saeedkazem@gmail.com (S. Kazem), k_parand@sbu.ac.ir (K. Parand).

0898-1221/$ – see front matter © 2012 Elsevier Ltd. All rights reserved.
doi:10.1016/j.camwa.2012.03.104

subject to

$$\ddot{X}(\tau) + \delta\dot{X}(\tau) + \omega^2 X(\tau) + \epsilon X^3(\tau) = f\cos(\alpha\tau) + U(\tau), \quad -T \le \tau \le 0, \tag{2}$$

where T is known, ω is the stiffness parameter, $\delta \ge 0$ is the viscous damping coefficient, f and α are the amplitude and frequency of the external input, respectively. Also the initial and boundary conditions are

$$X(-T) = x_0, \qquad X(0) = 0, \tag{3}$$

$$\dot{X}(-T) = x_1, \qquad \dot{X}(0) = 0. \tag{4}$$

The classical Duffing's equation was first introduced to study electronics and was published by Duffing in 1918 [4]. It is the simplest oscillator displaying catastrophic jumps of amplitude and phase when the frequency of the forcing term is taken as a gradually changing parameter. The Duffing equation has wide applications in signal processing [5], the propagation of extremely short electromagnetic pulses in a nonlinear medium [6,7], brain modeling [8], fuzzy modeling and the adaptive control of uncertain chaotic systems [9,10].

In classical development, it is well known that the variational method of optimal control theory, which typically consists of the calculus of variations and Pontryagin's methods [11], can be used to derive a set of necessary conditions that must be satisfied by an optimal control law and its associated state-control equations. These necessary optimality conditions lead to a (generally nonlinear) two-point boundary-value problem (2PBVP) that must be solved to determine an explicit expression for the optimal control. Except in some special cases, it is difficult to obtain the solution of this 2BVP and in some cases it is not practical to obtain it. In general, the solution of these distinct problems requires different numerical methods which will increase the computational time and effort.

Vlassenbroeck and Van Dooren [3] introduced a direct method for the controlled Duffing oscillator. In Vlassenbroeck et al. the state and control variables, the system dynamics, and the boundary conditions expanded in Chebyshev series of order m with unknown coefficients. In order to approximate the integral in the performance index, a summation of order m_1 was used, and in order to compute the integrand in the performance index, a summation of order $N > m_1$ was employed. Consequently, a rather complicated system of nonlinear equations have to be solved, for the unknowns, by some kind of iterative method.

A pseudospectral collocation method for solving the nonlinear controlled Duffing oscillator is presented in [12]. This approach is based on the idea of relating Legendre–Gauss–Lobatto collocation points to the structure of orthogonal polynomials.

Elnagar and Khamayseh [13] presented an alternative computational method for solving the controlled Duffing oscillator. Their approach drew upon the power of well-developed nonlinear programming techniques and computer codes to determine the optimal solutions of nonlinear systems. Central to the idea was a proper choice of trial functions, and the distribution of the collocation points is crucial to the accuracy of the solution. Thus, they constructed the Mth-degree interpolating polynomial using Chebyshev nodes as the collocation points and Lagrange polynomials as the trial functions to approximate the state and the control vectors.

El-Kady and Elbarbary [14] used Chebyshev polynomials for solving controlled Duffing oscillator. In [14], the control and state variables are approximated by Chebyshev series of different orders. The system dynamics, boundary conditions and performance index are approximated by using an explicit formula for the Chebyshev polynomials in terms of arbitrary order of their derivatives and a large system of nonlinear equations have to be solved.

Recently, Marzban and Razzaghi [15] have introduced an alternative computational method for solving the controlled Duffing oscillator. This method consists of reducing the controlled Duffing oscillator problem to a set of algebraic equations by expanding the second derivative of the state vector $\ddot{X}(\tau)$ and the control vector $U(\tau)$ as hybrid functions with unknown coefficients. These hybrid functions are consist of block-pulse functions and Legendre polynomials.

More recently, Lakestani et al. [16] have presented an alternative computational method for solving the controlled Duffing oscillator. Their method consists of reducing the controlled Duffing oscillator problem to a set of algebraic equations by using compactly supported linear B-spline wavelets, specially constructed for the bounded interval.

In this paper, a new computational method based on radial basis functions (RBFs) is introduced to solve the controlled Duffing oscillator. In this regard, in order to simplify the numerical integration method the Legendre–Gauss–Lobatto points for RBFs center nodes are applied, then the Lagrange multipliers method is employed to obtain optimum of the problem.

1.2. Introduction of the radial basis functions

The interpolation of data on scattered points, like those obtained by mesh based schemes, such as the boundary element method (BEM) and the finite element method (FEM) is a current problem. Conventional methods such as polynomial and spline interpolations have been handled to a comprehensive range of engineering problems. Alternatively, a radial basis functions (RBFs) interpolation can be applied for such a purpose.

RBFs was first studied by Roland Hardy, an Iowa State geodesist, in 1968. This method allows scattered data to be easily used in computations. An extensive study of interpolation methods available at the time was conducted by Franke [17], and concluded that RBFs interpolations were the most accurate techniques evaluated. The theory of RBFs has originated as a means to prepare a smooth interpolation of a discrete set of data points. The concept of using RBFs for solving DEs was first

Table 1
Some well-known functions that generate RBFs ($r = \|x - x_i\| = r_i$), $c > 0$.

Name of functions	Definition
Multiquadrics (MQ)	$\sqrt{r^2 + c^2}$
Inverse multiquadrics (IMQ)	$1/(\sqrt{r^2 + c^2})$
Gaussian (GA)	$\exp(-c^2 r^2)$
Inverse quadrics	$1/(r^2 + c^2)$

introduced by Kansa [18,19] who directly collocated the radial basis functions for the approximate solution of differential equations. However, in recent years RBFs have been extensively researched and applied in a wider range of analysis. Partial differential equations (PDEs) and ordinary differential equations (ODEs) have been solved using RBFs with recent work [20–42].

Recently, Kansa's method has been extended to solve various ordinary and partial differential equations including the nonlinear Klein–Gordon equation [24], regularized long wave (RLW) equation [28], high order ordinary differential equations [43], the case of heat transfer equations [27], Hirota–Satsuma coupled KdV equations [44], second-order parabolic equation with nonlocal boundary conditions [45], Second-order hyperbolic telegraph equation [46], one-dimensional wave equation with an integral condition [47], Lane–Emden-type equations [48], two-dimensional reaction–diffusion Brusselator system [49], nonhomogeneous Cauchy problems [50] and so on. An RBF $\Phi(\|X - X_i\|) : \mathbb{R}^+ \longrightarrow \mathbb{R}$ depends on the separation between a field point $X \in \mathbb{R}^d$ and the data centers X_i, for $i = 1, 2, \ldots, N$, and N data points. The interpolants are classed as radial due to their spherical symmetry around centers X_i, where $\|.\|$ is the Euclidean norm. The most known smooth RBFs are listed in Table 1 where $r = \|X - X_i\|$ and c is a free positive parameter, often referred to as the shape parameter, to be specified by the user. The shape parameter c within the Gaussian (GA) and multiquadric RBFs requires fine tuning and can dramatically alter the quality of the interpolation. Too large or too small shape parameter c make the GA too flat or too peaked. Despite many studies conducted to find algorithms for selecting the optimum values of c [51–55], the optimal choice of shape parameter is an open problem which is still under intensive investigation.

In the cases of inverse quadratic, inverse multiquadric (IMQ) and Gaussian (GA), the coefficient matrix of RBFs interpolate is positive definite and also, it has one positive eigenvalue and the remaining ones are all negative for multiquadric (MQ) [56].

The recent books and paper written by Buhmann [57,58] and Wendland [59] also provide helpful details about RBFs and their convergence rate.

In the current paper, we use the Gaussian (GA) radial basis functions to find the solution of the main problem. Also, to simplify the solution, we use the GA-RBF with Legendre–Gauss–Lobatto nodes as collocation nodes $\{x_j\}_{j=0}^{N}$.

This paper is arranged as follows. In Section 2, we present a brief formulation of the problem. In Section 3, we describe the properties of radial basis functions. In Section 4, the Legendre–Gauss–Lobatto nodes and weights are described. In Section 5, the collocation method based on RBFs is applied to solve the problem. In Section 6, we report our numerical findings and show the accuracy of the proposed method. The conclusions are discussed in the final Section.

2. The exact solution of controlled linear oscillator

Consider the optimal control problem of a linear oscillator given in [3,12,14]

$$J = \frac{1}{2}\int_{-T}^{0} U^2(\tau)d\tau, \tag{5}$$

subject to

$$\ddot{X}(\tau) + \omega^2 X(\tau) = U(\tau), \quad -T \le \tau \le 0, \tag{6}$$

where T is known, with

$$\begin{aligned} &X(-T) = x_0, \qquad X(0) = 0,\\ &\dot{X}(-T) = x_1, \qquad \dot{X}(0) = 0. \end{aligned} \tag{7}$$

Eqs. (6)–(7) are equivalent to

$$\dot{X}_1(\tau) = X_2(\tau), \qquad \dot{X}_2(\tau) + \omega^2 X_1(\tau) = U(\tau), \tag{8}$$

$$X_1(-T) = x_0, \qquad X_1(0) = 0, \tag{9}$$

$$X_2(-T) = x_1, \qquad X_2(0) = 0. \tag{10}$$

The problem is to find the control vector $U(\tau)$ which minimizes Eq. (5) subject to Eqs. (8)–(10). The exact solution of the controlled linear oscillator can be obtained by applying Pontryagin's maximum principle [11]

$$X_1(\tau) = \frac{1}{2\omega^2}[A_1\omega\tau\sin(\omega\tau) + A_2(\sin(\omega\tau) - \omega\tau\cos(\omega\tau))],$$

$$X_2(\tau) = \frac{1}{2\omega}[A_1(\sin(\omega\tau + \omega\tau\cos(\omega\tau))) + A_2\omega\tau\sin(\omega\tau)],$$
$$U(\tau) = A_1\cos(\omega\tau) + A_2\sin(\omega\tau),$$
$$J = \frac{1}{8\omega}[2\omega T(A_1^2 + A_2^2) + (A_1^2 - A_2^2)\sin(2\omega T) - 4A_1A_2\sin^2(\omega\tau)], \tag{11}$$

where

$$A_1 = \frac{2\omega[x_0\omega^2 T\sin(\omega T) - x_1(\omega T\cos(\omega T) - \sin(\omega T))]}{\omega^2T^2 - \sin^2(\omega T)},$$
$$A_2 = \frac{2\omega^2[x_1 T\sin(\omega T) + x_0(\sin(\omega T) + \omega T\cos(\omega T))]}{\omega^2T^2 - \sin^2(\omega T)}.$$

3. Radial basis functions

3.1. Definition of the radial basis functions

Let $\mathbb{R}^+ = \{x \in \mathbb{R}, x \geq 0\}$ be the non-negative half-line and let $\phi : \mathbb{R}^+ \to \mathbb{R}$ be a continuous function with $\phi(0) \geq 0$. A radial basis function on $\mathbb{R}^d$ is a function of the form

$$\phi(\|X - X_i\|),$$

where $X,\ X_i \in \mathbb{R}^d$ and $\|.\|$ denotes the Euclidean distance between X and X_is. If one chooses N points $\{X_i\}_{i=1}^N$ in $\mathbb{R}^d$ then by custom

$$s(X) = \sum_{i=1}^{N} \lambda_i\phi(\|X - X_i\|); \quad \lambda_i \in \mathbb{R},$$

is called a radial basis function as well [60].

The standard radial basis functions are categorized into two major classes [44].

Class 1. Infinitely smooth RBFs [44,47].

These basis functions are infinitely differentiable and heavily depend on the shape parameter c e.g. Hardy multiquadric (MQ), Gaussian(GA), inverse multiquadric (IMQ), and inverse quadric (IQ) (see Table 1).

Class 2. Infinitely smooth (except at centers) RBFs [44,47].

The basis functions of this category are not infinitely differentiable. These basis functions are shape parameter free and have comparatively less accuracy than the basis functions discussed in the Class 1. such as, thin plate spline, etc [44].

3.2. RBFs interpolation

The one dimensional function $y(x)$ can be approximated by an RBF as

$$y(x) \approx y_N(x) = \sum_{i=1}^{N} \lambda_i\phi_i(x) = \boldsymbol{\Phi}^T(x)\boldsymbol{\Lambda}, \tag{12}$$

where

$$\phi_i(x) = \varphi(\|x - x_i\|),$$
$$\boldsymbol{\Phi}^T(x) = [\phi_1(x), \phi_2(x), \ldots, \phi_N(x)],$$
$$\boldsymbol{\Lambda} = [\lambda_1, \lambda_2, \ldots, \lambda_N]^T, \tag{13}$$

x is the input and $\{\lambda_i\}_{i=1}^N$ are the set of coefficients that must be determined. By choosing N interpolation nodes $\{x_i\}_{i=1}^N$, we can approximate the function $y(x)$.

$$y_j = \sum_{i=1}^{N} \lambda_i\phi_i(x_j), \quad j = 1, 2, \ldots, N.$$

To summarize the discussion on coefficient matrix, we define:

$$\mathbf{A}\boldsymbol{\Lambda} = \mathbf{Y},$$

where

$$\begin{aligned}\mathbf{Y} &= [y_1, y_2, \ldots, y_N]^T,\\ \mathbf{A} &= [\boldsymbol{\Phi}^T(x_1), \boldsymbol{\Phi}^T(x_2), \ldots, \boldsymbol{\Phi}^T(x_N)]^T,\\ &= \begin{bmatrix} \phi_1(x_1) & \phi_2(x_1) & \ldots & \phi_N(x_1)\\ \phi_1(x_2) & \phi_2(x_2) & \ldots & \phi_N(x_2)\\ \vdots & \vdots & \ddots & \vdots\\ \phi_1(x_N) & \phi_2(x_N) & \ldots & \phi_N(x_N)\end{bmatrix}.\end{aligned} \tag{14}$$

Note that $\phi_i(x_j) = \varphi(\|x_j - x_i\|)$; therefore we have $\phi_i(x_j) = \phi_j(x_i)$, then $\mathbf{A} = \mathbf{A}^T$.

The infinitely smooth RBFs choices listed in Table 1 give coefficient matrices $\mathbf{A}$ in Eq. (14) which are symmetric and nonsingular [56], i.e. there is an unique interpolant of the form Eq. (12) no matter how the distinct data points are scattered in any number of space dimensions. In the cases of inverse quadratic, inverse multiquadric (IMQ), hyperbolic secant (sech), Gaussian (GA), the matrix $\mathbf{A}$ is positive definite and, for multiquadric (MQ), it has one positive eigenvalue and the remaining ones are all negative [56].

4. Legendre–Gauss–Lobatto nodes and weights

Let $\mathcal{H}_N[-1, 1]$ denote the space of algebraic polynomials of degree $\leq N$

$$\langle P_i, P_j\rangle = \frac{2}{2j+1}\delta_{ij}. \tag{15}$$

Here, $\langle ., .\rangle$ denotes the usual $L^2[-1, 1]$ inner product and $\{P_i\}_{i\geq 0}$ are the well-known Legendre polynomials of order i, which are orthogonal with respect to the weight function $w(x) = 1$ on the interval $[-1, 1]$, and satisfy the following recursive formulas:

$$\begin{aligned}&P_0(x) = 1, \qquad P_1(x) = x,\\ &P_{i+1}(x) = \left(\frac{2i+1}{i+1}\right)xP_i(x) - \left(\frac{i}{i+1}\right)P_{i-1}(x), \quad i = 1, 2, 3, \ldots.\end{aligned}$$

Next, we let $\{x_j\}_{j=0}^N$ as:

$$\begin{aligned}&(1 - x_j^2)\dot{P}_N(x_j) = 0,\\ &-1 = x_0 < x_1 < x_2 < \cdots < x_N = 1,\end{aligned} \tag{16}$$

where $\dot{P}_N(x)$ is a derivative of $P_N(x)$. No explicit formula for the nodes $\{x_j\}_{j=1}^{N-1}$ is known. However, they are computed numerically using the existing subroutines [61,62]. Now, we assume $f \in \mathcal{H}_{2N-1}[-1, 1]$, we have

$$\int_{-1}^{1} f(x)dx \simeq \sum_{j=0}^{N} \omega_j f(x_j) = \mathbf{I}_G(f), \tag{17}$$

where ω_j are the Legendre–Gauss–Lobatto weights, given in [63]

$$\omega_j = \frac{2}{N(N+1)} \times \frac{1}{(P_N(x_j))^2}. \tag{18}$$

5. Solving the controlled nonlinear Duffing oscillator

At first, we use the following transformations to convert the interval $[-T, 0]$ to $[-1, 1]$, then we use the numerical integration method, given in Eq. (17)

$$t = 1 + \frac{2}{T}\tau. \tag{19}$$

Therefore, the optimal control problem can be restated as follows

$$\frac{4}{T^2}\ddot{X}(t) + \frac{2}{T}\delta\dot{X}(t) + \omega^2 X(t) + \epsilon X^3(t) = f\cos(\alpha t) + U(t), \quad -1 \leq t \leq 1, \tag{20}$$

with boundary conditions

$$X(-1) = x_0, \qquad X(1) = 0, \tag{21}$$

$$\dot{X}(-1) = \frac{T}{2}x_1, \qquad \dot{X}(1) = 0. \tag{22}$$

Now, the problem is to find the optimal control $U(t)$ that minimizes the following cost functional:

$$J = \frac{T}{4}\int_{-1}^{1} U^2(t)dt. \tag{23}$$

In order to solve the problem, we approximate $X(t)$ and $U(t)$ by RBFs as:

$$X(t) \simeq X_N(t) = \sum_{k=0}^{N} \lambda_k^{[1]}\phi(\|t - t_k\|), \tag{24}$$

$$U(t) \simeq U_N(t) = \sum_{k=0}^{N} \lambda_k^{[2]}\phi(\|t - t_k\|), \tag{25}$$

where $\phi(\|t - t_i\|) = e^{-c^2(t-t_i)^2}$, $-1 \le t_i \le 1$ and $i = 0, 1, \ldots, N-1, N$.

Center nodes $\{t_i\}_{i=0}^{N}$ are chosen as:

$$\begin{aligned} &(1 - t_i^2)\dot{P}_N(t_i) = 0,\\ &-1 = t_0 < t_1 < t_2 < \cdots < t_N = 1, \end{aligned} \tag{26}$$

where $\dot{P}_N(t)$ is the derivative of $P_N(t)$. We define residual functions $Res(t)$ by substituting Eq. (24), and (25) in Eq. (20)

$$Res(t) = \frac{4}{T^2}\frac{d^2}{dt^2}X_N(t) + \frac{2\delta}{T}\frac{d}{dt}X_N(t) + \omega^2 X_N(t) + \epsilon X_N^3(t) - f\cos(\alpha t) - U_N(t). \tag{27}$$

The boundary conditions of the problem are obtained as

$$\begin{cases} X_N(-1) \approx x_0,\\ X_N(1) \approx 0,\\ \dfrac{d}{dt}X_N(t)\mid_{t=-1} \approx \dfrac{T}{2}x_1,\\ \dfrac{d}{dt}X_N(t)\mid_{t=1} \approx 0. \end{cases} \tag{28}$$

Then, we use $N+1$ collocation nodes which are the same as the number of center nodes. Subsequently, a set of nonlinear algebraic equations is constructed by using Eq. (27) together with the conditions in Eq. (28)

$$F_i = Res(t_i) = \frac{4}{T^2}\frac{d^2}{dt^2}X_N(t_i) + \frac{2\delta}{T}\frac{d}{dt}X_N(t_i) + \omega^2 X_N(t_i) + \epsilon X_N^3(t_i) - f\cos(\alpha t_i) - U_N(t_i), \tag{29}$$

where $i = 0, 1, \ldots, N-1, N$ and also we have

$$\begin{cases} F_{N+1} = X_N(-1) - x_0,\\ F_{N+2} = X_N(1),\\ F_{N+3} = \dfrac{d}{dt}X_N(t)\mid_{t=-1} - \dfrac{T}{2}x_1,\\ F_{N+4} = \dfrac{d}{dt}X_N(t)\mid_{t=-1}. \end{cases} \tag{30}$$

Next we approximate the cost functional Eq. (23) as

$$J = \frac{T}{4}\int_{-1}^{1} U_N^2(t)dt, \tag{31}$$

$$\approx \frac{T}{4}\sum_{r=0}^{M_1} \omega_r U_N^2(t_r), \tag{32}$$

where $\{t_r\}_{r=0}^{M_1}$ are given in Eq. (16) and also ω_r is given in Eq. (18). Thus, the optimal control problem is reduced to a parameter optimization problem which is stated as follows.

Find $\boldsymbol{\Lambda}^{[1]} = \{\lambda_0^{[1]}, \lambda_1^{[1]}, \ldots, \lambda_N^{[1]}\}$ and $\boldsymbol{\Lambda}^{[2]} = \{\lambda_0^{[2]}, \lambda_1^{[2]}, \ldots, \lambda_N^{[2]}\}$ which minimize Eqs. (29), (30) and (32). To find $\boldsymbol{\Lambda}^{[1]}$ and $\boldsymbol{\Lambda}^{[2]}$, we define

$$L(\boldsymbol{\Lambda}^{[1]}, \boldsymbol{\Lambda}^{[2]}, \boldsymbol{\Gamma}^{[1]}) = J + \sum_{k=0}^{N+4} \gamma_k F_k, \tag{33}$$

Table 2
Estimated and exact values of $X(\tau)$ and $U(\tau)$ for $N = 10$ and 15 of Example 1.

	$X(\tau)$			$U(\tau)$		
τ	$N = 10$	$N = 15$	Exact	$N = 10$	$N = 15$	Exact
−2.0	0.50000000	0.50000000	0.50000000	0.48758907	0.48896678	0.48896700
−1.5	0.26277013	0.26277310	0.26277310	0.54951140	0.54918928	0.54918927
−1.0	0.09285795	0.09285787	0.09285787	0.47496222	0.47495086	0.47495085
−0.5	0.01406189	0.01405957	0.01405957	0.28418112	0.28442789	0.28442790
0.0	0.00000000	0.00000000	0.00000000	0.02520254	0.02426723	0.02426707

where $\boldsymbol{\Gamma}^{[1]} = \{\gamma_0, \gamma_1, \ldots, \gamma_{N+4}\}$ are Lagrange multipliers. The necessary conditions for a minimization problem are

$$\frac{\partial L}{\partial \lambda_k^{[1]}} = 0, \quad k = 0, 1, \ldots, N, \tag{34}$$

$$\frac{\partial L}{\partial \lambda_k^{[2]}} = 0, \quad k = 0, 1, \ldots, N, \tag{35}$$

$$\frac{\partial L}{\partial \gamma_k} = F_k = 0, \quad k = 0, 1, \ldots, N + 4. \tag{36}$$

Eqs. (34)–(36) produce a system of nonlinear algebraic equations which can be solved by a mathematical software for the unknowns $\boldsymbol{\Lambda}^{[1]}$, $\boldsymbol{\Lambda}^{[2]}$ and $\boldsymbol{\Gamma}^{[1]}$. Although, it is worth mentioning that it is too difficult to solve this system of nonlinear equations even by Newton's method. The main difficulty with such a system is, how we can choose initial guess to handle Newton's method; in other words, how many solutions the system of nonlinear equations admit. We think the best way to discover a proper initial guess (or initial guesses) is to solve the system analytically for very small N (by using symbolic software programs such as Mathematica or Maple), and then we can find proper initial guesses, particularly multiplicity of solutions of such system. This action has been done by starting from proper initial guesses with the maximum number of ten iterations.

6. The numerical results

In order to illustrate the performance of the RBFs method in solving the controlled nonlinear Duffing oscillator and justify the accuracy and efficiency of the method presented in this research, we consider the following examples. In all examples, we use the Gaussian (GA) RBF for $c = 1$ and various values of N. The numerical implementation is carried out in microsoft.maple.13, with hardware configuration: desktop Intel Core 2 Duo CPU, 4 GB of RAM.

6.1. Example 1

Consider Eqs. (1)–(3) with

$$\omega = 1, \quad T = 2, \quad \epsilon = 0, \quad f = 0, \quad \delta = 0,$$
$$\alpha = 0.5, \quad x_0 = 0.5, \quad x_1 = -0.5 \tag{37}$$

which have the exact solutions

$$X(\tau) = \frac{\sin(2) + 2\cos(2)}{2(4 - \sin^2(2))}\tau \sin(\tau) + \frac{2\cos(2) - \sin(2)}{2(4 - \sin^2(2))}(\sin(\tau) - \tau\cos(\tau)),$$
$$U(\tau) = \frac{2\cos(2) - \sin(2)}{4 - \sin^2(2)} \sin(\tau) + \frac{\sin(2) + 2\cos(2)}{4 - \sin^2(2)} \cos(\tau). \tag{38}$$

In Table 2, a comparison is made between the values of $X(\tau)$ and $U(\tau)$ using the present method for $N = 10$ and 15, the exact solutions in the standard case Eq. (37) for $-2 \le \tau \le 0$.

In Table 3, a comparison is made between the present method for $N = 4, 6, 8, \ldots, 18, 20$ together with the solution obtained by Dooren and Vlassenbroeck [3], the Legendre Pseudospectral method [12] and the Chebyshev Pseudospectral method [13] for the controlled linear oscillator and the exact solution. We report the absolute errors ($|J_{exact} - J_{implicit}|$), where $J_{implicit}$ is obtained from the present method, J_{exact} is the exact solution of the problem in Eq. (11), $\|Res(\tau)\|_2$ and the CPU time (s), which represents the time required to attain such precision. As N increases, the absolute errors ($|J_{exact} - J_{implicit}|$) and $\|Res(\tau)\|_2$ decrease significantly and the results will rapidly tend to the exact values. This table illustrates that the present method has a good convergence rate.

The solutions are presented graphically in Fig. 1. In Fig. 1 we compared the present method and exact solution of $X(\tau)$ and $U(\tau)$. The absolute errors ($|X_{exact}(\tau) - X_{implicit}(\tau)|$) and ($|U_{exact}(\tau) - U_{implicit}(\tau)|$) are presented graphically in Fig. 2(a),(b) respectively. These figures show the decreasing absolute error by the collocation method based on the GA-RBF.

Finally, the phase portrait behavior of the controlled Duffing oscillator is shown in Fig. 3.

Table 3
Estimated and exact values of J for Example 1.

Methods	J	$\lvert J_{implicit} - J_{exact}\rvert$	$\lVert Res(\tau)\rVert_2$	CPU time (s)
Method of [3]				
$M = 4.0$	0.184917			
$M = 7.0$	0.18485854			
$M = 10$	0.1848585424			
Legendre pseudospectral method [12]				
$M = 4.0$	0.184871			
$M = 6.0$	0.184858554			
$M = 8.0$	0.1848585424			
Chebyshev pseudospectral method [13]				
$M = 5.0$	0.18485871			
$M = 6.0$	0.1848585424			
Present method				
$N = 4.0$	0.223031934020577	3.81733e−02	6.02e−02	0.406
$N = 6.0$	0.186100046239558	1.24150e−03	7.70e−03	0.468
$N = 8.0$	0.184867276203868	8.73384e−06	6.01e−04	0.546
$N = 10$	0.184858593684025	5.13202e−08	3.69e−05	0.577
$N = 12$	0.184858542491256	1.27481e−10	1.71e−06	0.640
$N = 14$	0.184858542364041	2.66488e−13	9.09e−08	0.687
$N = 16$	0.184858542363774	3.21039e−16	2.65e−09	0.795
$N = 18$	0.184858542363774	3.16185e−19	6.61e−11	0.873
$N = 20$	0.184858542363774	2.21955e−22	1.47e−12	0.967
Exact	0.184858542363774			

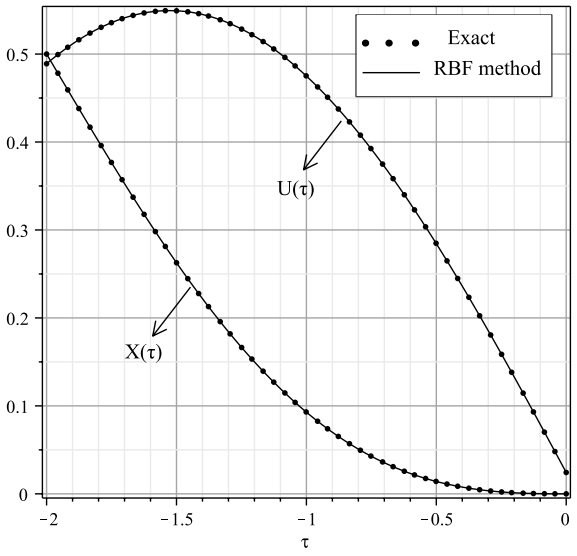

Fig. 1. Graph of numerical approximates $X(\tau)$ and $U(\tau)$ by using the Gaussian RBF and an exact solution with $N = 15$ for Example 1.

6.2. Example 2

Consider Eqs. (1)–(3) with

$$\omega = 0.7, \quad T = 25, \quad \epsilon = 0, \quad f = 1, \quad \delta = 0.2,$$
$$\alpha = 2, \quad x_0 = 2, \quad x_1 = -2. \tag{39}$$

Since there is no exact solution of this example, we show the convergency of the RBFs method by using the residual error norm in Table 5 and Fig. 5. The table and figure show that the RBFs method is an accurate method for solving this problem. In Table 4, a comparison is made between the values of $X(\tau)$ and $U(\tau)$ using the present method in $N = 14, 17, 20$ for $-25 \leq \tau \leq 0$. In Table 5, we report ($J_{implicit}$) for the controlled nonlinear oscillator, where $J_{implicit}$ is obtained from the present method for $N = 10, 12, \ldots, 18, 20$. The solutions are presented graphically in Fig. 4. Also, the residual functions $Res(\tau)$ are presented graphically in Fig. 5. Finally, the phase portrait behavior of the controlled Duffing oscillator is shown in Fig. 6.

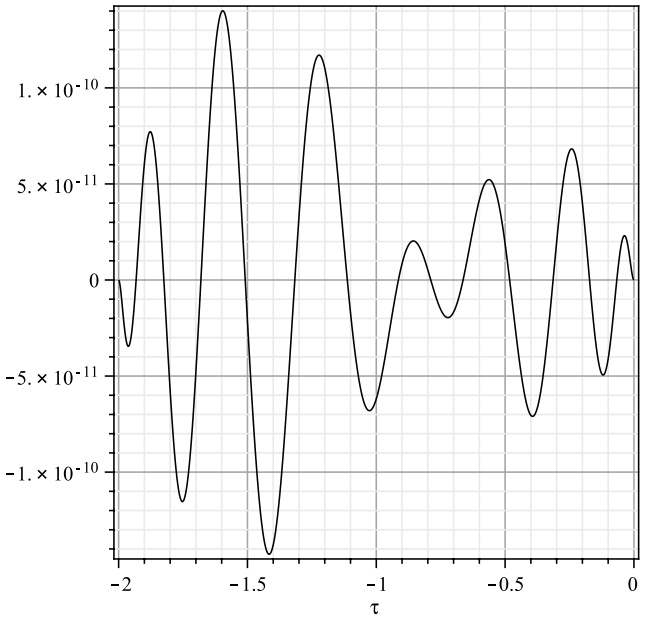

(a) Absolute error of $X(\tau)$.

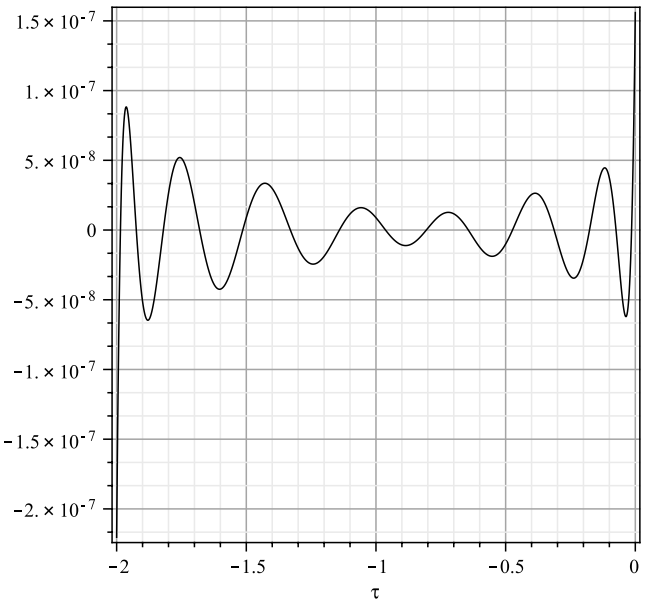

(b) Absolute error of $U(\tau)$.

Fig. 2. Graph of the absolute error between the GA-RBF solution and the exact solution of $X(\tau)$ and $U(\tau)$ with $N = 15$ for Example 1.

Table 4
Estimated values of $X(\tau)$ and $U(\tau)$ for $N = 14$, 17 and 20 of Example 2.

τ	$X(\tau)$			$U(\tau)$		
	$N = 14$	$N = 17$	$N = 20$	$N = 14$	$N = 17$	$N = 20$
−25	2.00000000	2.00000000	2.00000000	−0.01003639	−0.01082365	−0.01080628
−20	−0.54952497	−0.54946175	−0.54945952	0.02019462	0.02025857	0.02025604
−15	2.14035650	2.14037525	2.14038178	−0.03409742	−0.03396664	−0.03397531
−10	2.28370969	2.28343598	2.28344244	0.05096086	0.05120262	0.05119398
−5	0.39749187	0.39729546	0.39729639	−0.06797934	−0.06775068	−0.06775186
0	0.00000000	0.00000000	0.00000000	0.071871100	0.07270446	0.07272936

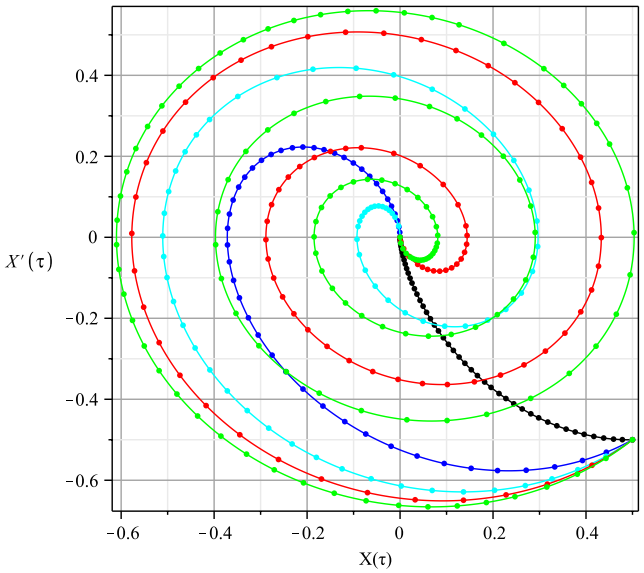

Fig. 3. Phase portrait of the controlled Duffing oscillator with $N = 15$ for Example 1. $T = 2$ (Black), $T = 5$ (Blue), $T = 10$ (Cyan), $T = 15$ (Red), and $T = 20$ (Green). (For interpretation of the references to colour in this figure legend, the reader is referred to the web version of this article.)

Table 5
Estimated values of J for Example 2.

N	J	$\|Res(\tau)\|_2$	CPU time (s)
10	0.041671380723755	2.87e−03	0.593
12	0.032301910331246	1.66e−03	0.671
14	0.032288596461730	1.95e−04	0.718
16	0.032287080276060	1.93e−06	0.827
18	0.032287052748995	3.81e−07	1.014
20	0.032287052713585	1.02e−09	1.123

Table 6
Estimated values of $X(\tau)$ and $U(\tau)$ for $N = 13$, 14 and 15 of Example 3.

τ	$X(\tau)$			$U(\tau)$		
	$N = 13$	$N = 14$	$N = 15$	$N = 13$	$N = 14$	$N = 15$
−5	1.00000000	1.00000000	1.00000000	0.32504074	0.32825552	0.33025768
−4	0.06421073	0.06422713	0.06422568	0.16391774	0.16293815	0.16299639
−3	−0.28626772	−0.28624338	−0.28624233	−0.21192495	−0.21308116	−0.21307268
−2	−0.19948612	−0.19947263	−0.19946567	−0.51147270	−0.51221989	−0.51244984
−1	−0.04351429	−0.04350950	−0.04350536	−0.55008328	−0.55047293	−0.55064934
0	0.00000000	0.00000000	0.00000000	−0.30255554	−0.30061369	−0.30189402

6.3. Example 3

Consider the nonlinear case of Eqs. (1)–(3) with

$$\omega = 0.7, \quad T = 5, \quad \epsilon = 1, \quad f = 0.5, \quad \delta = 0.2, \quad \alpha = 1,$$
$$x_0 = 1, \quad x_1 = -1. \tag{40}$$

Since there is no exact solution of this problem, we show the convergency of the RBFs method by using the residual error norm in Table 7 and Fig. 8. In Table 6, a comparison is made between the values of $X(\tau)$ and $U(\tau)$ using the present method in $N = 13$, 14 and 15 for $-5 \leq \tau \leq 0$. In Table 7, we report ($J_{implicit}$) for the controlled nonlinear oscillator, where $J_{implicit}$ is obtained from the present method for $N = 10, 12, \ldots, 18, 20$. The solutions are presented graphically in Fig. 7. Also, the residual functions $Res(\tau)$ are presented graphically in Fig. 8. Finally, the phase portrait behavior of the controlled Duffing oscillator is shown in Fig. 9.

7. Conclusions

In this research, some new ideas have been represented for optimal linear and nonlinear control design of the nonlinear controlled Duffing oscillator system. We proposed a numerical method based on radial basis functions for solving the

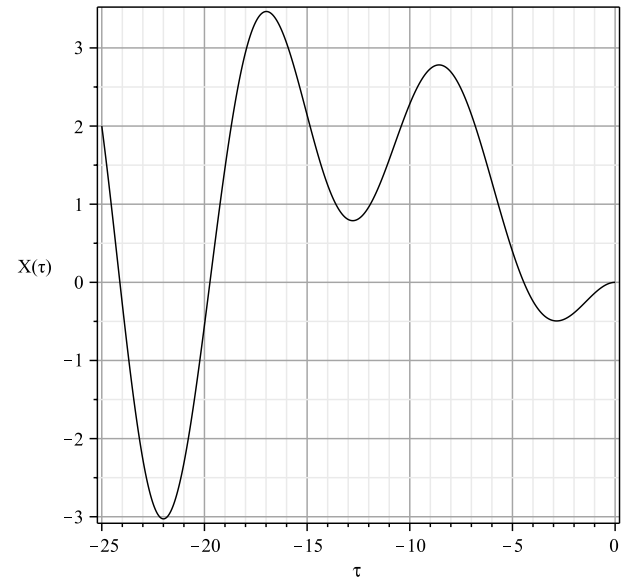

(a) $X(\tau)$.

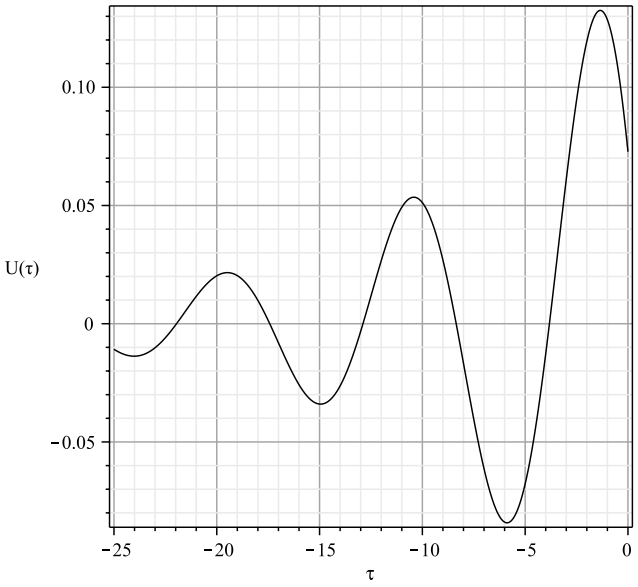

(b) $U(\tau)$.

Fig. 4. Graph of numerical approximates $X(\tau)$ and $U(\tau)$ by using the Gaussian RBF and the exact solution with $N = 15$ for Example 2.

Table 7
Estimated values of J for Example 3.

N	J	$\|Res(\tau)\|_2$	CPU time (s)
10	0.382404639075082	6.32e−03	4.103
12	0.382393141318598	1.31e−03	7.144
14	0.382390057527092	1.54e−04	13.868
16	0.382389694236828	5.71e−05	22.230
18	0.382389692004907	1.39e−05	32.510
20	0.382389691680160	9.92e−07	49.202

optimal control of a nonlinear controlled Duffing oscillator. The controlled nonlinear Duffing oscillator is known to describe many important oscillating phenomena in some nonlinear physical and engineering systems. RBFs are simple and practical methods to approximate functions. One of the main advantages of RBFs is that, they can work with different distribution

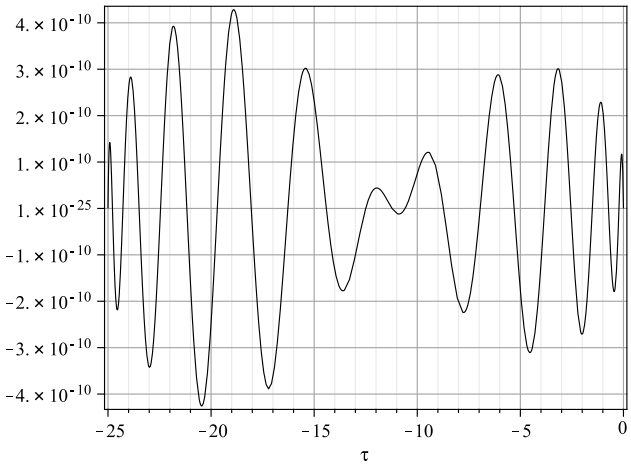

Fig. 5. Graph of $Res(\tau)$ by the GA-RBF solution with $N = 20$ of Example 2.

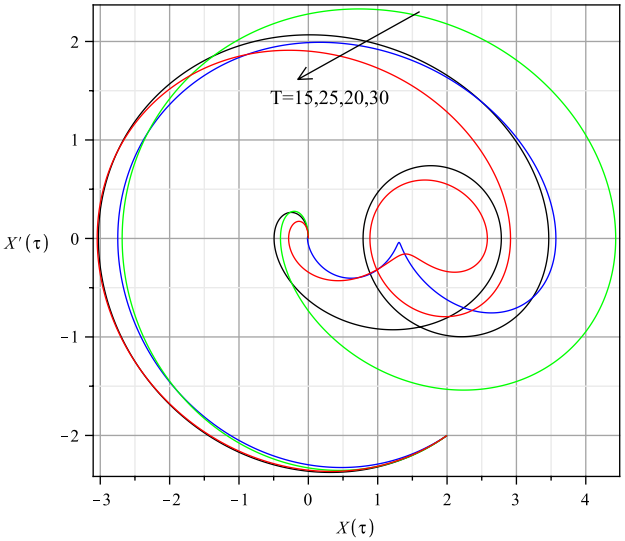

Fig. 6. Phase portrait of the controlled Duffing oscillator with $N = 20$ for Example 2.

Table 8
The residual norms and error $J_{implicit} - J_{exact}$ of the RBF method for some values of shape parameter when $N = 20$ in Example 1.

c	$\|Res(\tau)\|_2$	$J_{implicit} - J_{exact}$
2.0	5.38e−06	8.6489e−12
1.8	6.38e−07	3.5710e−13
1.6	5.45e−08	9.0020e−15
1.4	3.10e−09	9.4078e−17
1.2	1.02e−10	3.2851e−19
1.0	1.47e−12	2.2196e−22
0.8	3.21e−15	2.1519e−26
0.6	2.75e−17	2.6334e−30
0.4	8.68e−20	6.4889e−36
0.2	6.89e−25	1.0036e−43
0.1	1.14e−28	9.4258e−38
0.05	1.01e−34	6.2837e−28
0.01	1.48e−48	5.2965e−17

of points. In Fig. 10, we solve the above-mentioned examples by using tree different case of center nodes, Legendre nodes, Chebyshev nodes, and uniform distribution nodes. These figures show that by increasing N, the value of $\|Res(\tau)\|_2$ that is

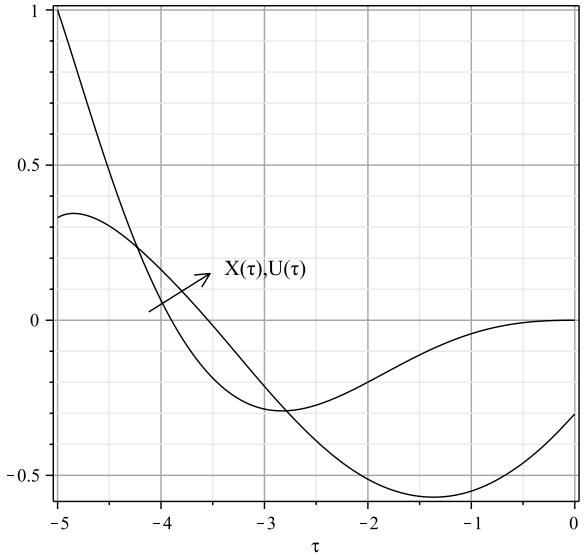

Fig. 7. Graph of numerical approximates $X(\tau)$ and $U(\tau)$ by using the Gaussian RBF and the exact solution with $N = 15$ for Example 3.

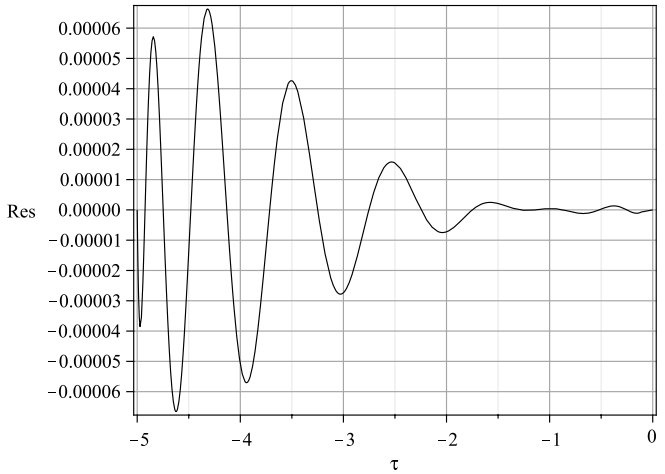

Fig. 8. Graph of $Res(\tau)$ by the GA-RBF solution with $N = 15$ of Example 3.

Table 9
The residual norms and the values $J_{implicit}$ of the RBF method for some values of the shape parameter when $N = 20$ in Example 2.

c	$\|Res(\tau)\|_2$	$J_{implicit}$
2.0	1.02e−05	0.03228705698305711865
1.8	2.19e−06	0.03228705244385156088
1.6	3.86e−07	0.03228705247835788099
1.4	2.03e−07	0.03228705269054206644
1.2	8.20e−09	0.03228705271345494651
1.0	1.02e−09	0.03228705271358529115
0.8	5.77e−09	0.03228705271403483624
0.6	1.37e−08	0.03228705271388723607
0.4	1.66e−08	0.03228705271614747252
0.2	1.60e−09	0.03228705362768460814
0.1	2.05e−18	0.03228952341489231153
0.05	5.46e−21	0.03253877886306246238

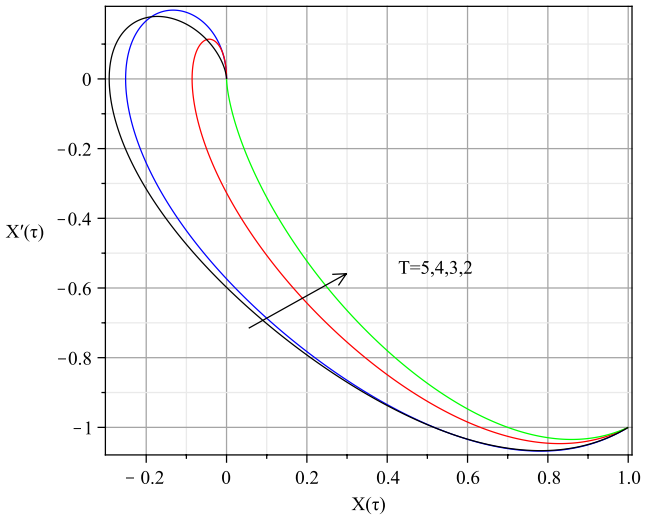

Fig. 9. Phase portrait of the controlled Duffing oscillator with $N = 15$ for Example 3.

Table 10
The residual norms and the values $J_{implicit}$ of the RBF method for some values of the shape parameter when $N = 20$ in Example 3.

c	$\|Res(\tau)\|_2$	$J_{implicit}$
2.0	1.40e−05	0.38238969180228517602
1.8	1.64e−05	0.38238969170247629936
1.6	1.11e−05	0.38238969166401008697
1.4	6.01e−06	0.38238969167787583912
1.2	2.72e−06	0.38238969168831772034
1.0	9.92e−07	0.38238969168016052849
0.8	4.35e−07	0.38238969166683519258
0.6	1.21e−07	0.38238969166607312423
0.4	8.87e−08	0.38238969167142410241
0.2	3.12e−08	0.38238969167435277102
0.1	1.91e−08	0.38238969167972112307

obtained by using Legendre nodes as the center nodes, decreases rapidly, and also this case has a good convergence rate. We convert the main problem to a set of nonlinear equations by expanding the candidate function with unknown coefficients; then the method of Lagrange multipliers is used to solve the problem.

Tables 8–10 are considered to illustrate the effect of the shape parameter c on RBF solutions. In these tables, the effect of shape parameter c on $\|Res(\tau)\|_2$ and the value of J is shown. The shape parameter c should be chosen to reduce the value of $\|Res(\tau)\|_2$ and also the minimum value of J. From Table 8, it can be seen that if the shape parameter is selected in the interval (0.2, 1), we have $\|Res(\tau)\|_2 < 10^{-10}$ and also $J_{implicit}$ and J_{exact} are equal to 22 decimal positions. In addition, Table 9 shows that if the shape parameter is selected in the interval (0.2, 1.6), we have $\|Res(\tau)\|_2 \leq 10^{-7}$, and also in this interval, the value of J does not change and correct to 9 decimal positions; $J_{implicit} \simeq 0.032287052$. Finally, from Table 10 it can be seen that if the shape parameter c is selected in the interval (0.1, 1.4), we have $\|Res(\tau)\|_2 \leq 10^{-6}$ and also in this interval, the value of J does not change and correct to 9 decimal positions; $J_{implicit} \simeq 0.382389691$.

The given examples show that using the present approach leads to acceptable results in comparison with different approximation methods. Finally, we note that the proposed method can be applied to a large class of nonlinear and chaotic systems [64–72].

Acknowledgments

We are very grateful to the two reviewers for carefully reading this paper and for their comments and suggestions which have improved the present paper. Also, we would like to acknowledge the Editor-in-Chief, Professor Ervin Y. Rodin, for managing the review process for this paper.

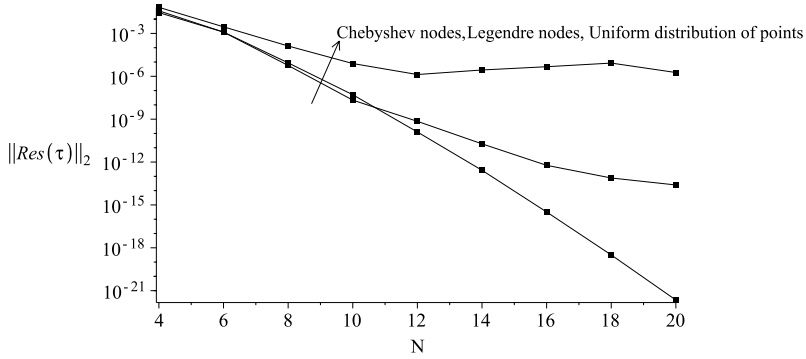

(a) Example 1.

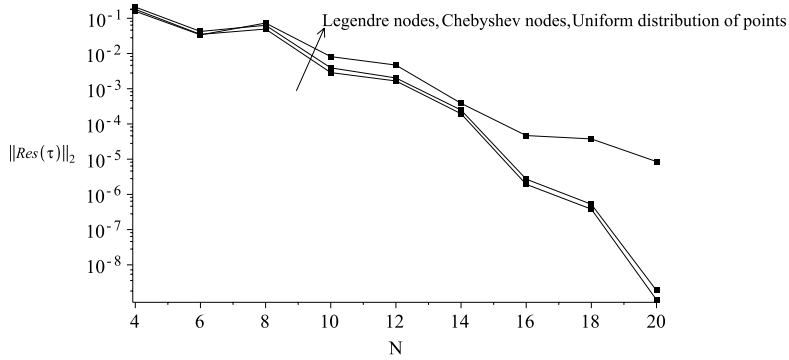

(b) Example 2.

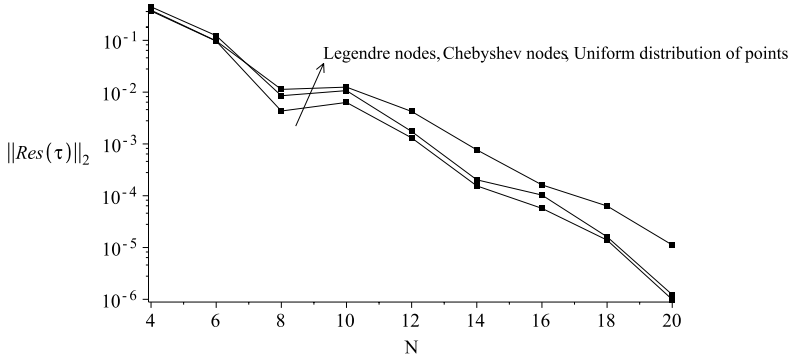

(c) Example 3.

Fig. 10. The RBF solution by using tree different case of center nodes, Legendre nodes, Chebyshev nodes and uniform distribution nodes.

References

[1] J.C. Gille, P. Decaulne, M. Pelegrain, Systems Asservis Non Lineaires, Bordas, Paris, 1975.
[2] A.H. Nayfeh, D.T. Mook, Nonlinear Oscillations, Wiley, New York, 1979.
[3] R.V. Dooren, J. Vlassenbroeck, Chebyshev series solution of the controlled duffing oscillator, J. Comput. Phys. 47 (1982) 321–329.
[4] J.J. Stokes, Nonlinear Vibrations, Intersciences, New York, 1950.
[5] G. Wang, W. Zhenga, S. He, Estimation of amplitude and phase of a weak signal by using the property of sensitive dependence on initial conditions of a nonlinear oscillator, Signal Process. 82 (2002) 103–115.
[6] A.I. Maimistov, Some models of propagation of extremely short electromagnetic pulses in a nonlinear medium, Quantum Electron. 30 (2000) 287–304.
[7] A.I. Maimistov, Propagation of an ultimately short electromagnetic pulse in a nonlinear medium described by the fifth-order duffing model, Opt. Spectrosc. 94 (2003) 251–257.
[8] E. Zeeman, Duffing equation in brain modelling, Bull. IMA 12 (1976) 207–214.
[9] M. Feki, Observer-based exact synchronization of ideal and mismatched chaotic systems, Phys. Lett. A 309 (2003) 53–60.
[10] B. Ravindra, A.K. Mallik, Dissipative control of chaos in non-linear vibrating systems, J. Sound Vib. 211 (1998) 709–715.
[11] L.S. Pontryagin, V. Boltyanskii, R. Gamkrelidze, E. Mischenko, The Mathematical Theory of Optimal Processes, Interscience, New York, 1962.
[12] M. Razzaghi, G. Elnagar, Numerical solution the controlled duffing oscillator by the pseudospectral method, J. Computat. Appl. Math. 56 (1994) 253–261.

[13] G. Elnagar, A. Khamayseh, On the optimal spectral Chebyshev solution of a controlled nonlinear dynamical system, IMA J. Appl. Math. 58 (1997) 147–157.
[14] M. El-kady, E.M.E. Elbarbary, A Chebyshev expansion method for solving nonlinear optimal control problems, Appl. Math. Comput. 129 (2002) 171–182.
[15] H.R. Marzban, M. Razzaghi, Numerical solution of the controlled duffing oscillator by hybrid functions, Appl. Math. Comput. 140 (2003) 179–190.
[16] M. Lakestani, M. Razzaghi, M. Dehghan, Numerical solution of the controlled duffing oscillator by semi-orthogonal spline wavelets, Phys. Scr. 74 (2006) 362–366.
[17] R. Franke, Scattered data interpolation: test of some methods, Math. Comput. 38 (1982) 181–200.
[18] E.J. Kansa, Multiquadrics-A scattered data approximation scheme with applications to computational fluid-dynamics-I surface approximations and partial derivative estimates, Comput. Math. Appl. 19 (1990) 127–145.
[19] E.J. Kansa, Multiquadrics—a scattered data approximation scheme with applications to computational fluid-dynamics-II solutions to parabolic, hyperbolic and elliptic partial differential equations, Comput. Math. Appl. 19 (1990) 147–161.
[20] M. Sharan, E.J. Kansa, S. Gupta, Application of the multiquadric method for numerical solution of elliptic partial differential equations, Appl. Math. Comput. 84 (1997) 275–302.
[21] M. Zerroukat, H. Power, C.S. Chen, A numerical method for heat transfer problems using collocation and radial basis functions, Int. J. Numer. Meth. Eng. 42 (1998) 1263–1278.
[22] N. Mai-Duy, T. Tran-Cong, Numerical solution of differential equations using multiquadric radial basis function networks, Neural Netw. 14 (2001) 185–199.
[23] M. Tatari, M. Dehghan, A method for solving partial differential equations via radial basis functions: application to the heat equation, Eng. Anal. Bound. Elem. 34 (2010) 206–212.
[24] M. Dehghan, A. Shokri, Numerical solution of the nonlinear Klein–Gordon equation using radial basis functions, J. Comput. Appl. Math. 230 (2009) 400–410.
[25] A. Alipanah, M. Dehghan, Numerical solution of the nonlinear Fredholm integral equations by positive definite functions, Appl. Math. Comput. 190 (2007) 1754–1761.
[26] S. Sarra, Adaptive radial basis function method for time dependent partial differential equations, Appl. Numer. Math. 54 (2005) 79–94.
[27] K. Parand, S. Abbasbandy, S. Kazem, A. Rezaei, Comparison between two common collocation approaches based on radial basis functions for the case of heat transfer equations arising in porous medium, Commun. Nonlinear. Sci. Numer. Simul. 16 (2010) 1396–1407.
[28] Siraj-ul-islam, S. Haqb, A. Ali, A meshfree method for the numerical solution of the RLW equation, J. Comput. Appl. Math. 223 (2009) 997–1012.
[29] A. Golbabai, M. Mammadova, S. Seifollahi, Solving a system of nonlinear integral equations by an RBF network, Comput. Math. Appl. 57 (2009) 1651–1658.
[30] S. Kazem, J.A. Rad, K. Parand, S. Abbasbandy, A new method for solving steady flow of a third grade fluid in a porous half space based on radial basis functions, Z. Naturforsch. A 66a (2011) 591–598.
[31] K. Parand, S. Abbasbandy, S. Kazem, J.A. Rad, A novel application of radial basis functions for solving a model of first-order integro-ordinary differential equation, Commun. Nonlinear. Sci. Numer. Simulat. 16 (2011) 4250–4258.
[32] G. Yao, Siraj-ul-islam, B. Sarler, A comparative study of global and local meshless methods for diffusion–reaction equation, Comput. Model. Eng. Sci. (CMES) 59 (2010) 127–154.
[33] Siraj-ul-islam, A. Ali, S. Haq, A computational modeling of the behavior of the two-dimensional reaction–diffusion Brusselator system, Appl. Math. Model. 34 (2010) 3896–3909.
[34] S. Kazem, J.A. Rad, K. Parand, Radial basis functions methods for solving Fokker–Planck equation, Eng. Anal. Bound. Elem. 36 (2012) 181–189.
[35] S. Kazem, J.A. Rad, Radial basis functions method for solving of a non-local boundary value problem with Neumann's boundary conditions, Appl. Math. Modell. 36 (2012) 2360–2369.
[36] S. Kazem, J.A. Rad, K. Parand, A meshless method on non-Fickian flows with mixing length growth in porous media based on radial basis functions, Comput. Math. Appl. (2011), http://dx.doi.org/10.1016/j.camwa.2011.10.052.
[37] K. Parand, J.A. Rad, Numerical solution of nonlinear Volterra–Fredholm–Hammerstein integral equations via collocation method based on radial basis functions, App. Math. Comput. 218 (2012) 5292–5309.
[38] Y. Dereli, Solitary Wave solutions of the MRLW equation using radial basis functions, Numer. Meth. Part. D. E. 28 (2012) 235–247.
[39] Y. Dereli, Radial basis functions method for numerical solution of the modified equal width equation, Int. J. Comput. Math. 87 (2010) 1569–1577.
[40] S.G. Ahmed, M.L. Mekey, A collocation and Cartesian grid methods using new radial basis function to solve class of partial differential equations, Int. J. Comput. Math. 87 (2010) 1349–1362.
[41] S.G. Ahmed, A collocation method using new combined radial basis functions of thin plate and multiquadraic types, Eng. Anal. Bound. Elem. 30 (2006) 697–701.
[42] R.-H. Wang, M. Xua, Q. Fang, A kind of improved univariate multiquadric quasi-interpolation operators, Comput. Math. Appl. 59 (2010) 451–456.
[43] N. Mai-Duy, Solving high order ordinary differential equations with radial basis function networks, Int. J. Numer. Meth. Eng. 62 (2005) 824–852.
[44] A.J. Khattak, S.I.A. Tirmizi, Siraj-ul-islam, Application of meshfree collocation method to a class of nonlinear partial differential equations, Eng. Anal. Bound. Elem. 33 (2009) 661–667.
[45] M. Dehghan, M. Tatari, Use of radial basis functions for solving the second-order parabolic equation with nonlocal boundary conditions, Numer. Meth. Part. D. E. 24 (2008) 924–938.
[46] M. Dehghan, A. Ghesmati, Solution of the second-order one-dimensional hyperbolic telegraph equation by using the dual reciprocity boundary integral equation (DRBIE) method, Eng. Anal. Bound. Elem. 34 (2010) 51–59.
[47] M. Dehghan, A. Shokri, A meshless method for numerical solution of the one-dimensional wave equation with an integral condition using radial basis functions, Numer. Algorithms 52 (2009) 461–477.
[48] K. Parand, S. Abbasbandy, S. Kazem, A.R. Rezaei, An improved numerical method for a class of astrophysics problems based on radial basis functions, Phys. Scr. 83 (2011) 015011.
[49] Siraj-ul-islam, A. Ali, S. Haq, A computational modeling of the behavior of the two-dimensional reaction–diffusion Brusselator system, Appl. Math. Model. 34 (2010) 3896–3909.
[50] M. Lia, C. Chenb, Y. Hon, A meshless method for solving nonhomogeneous Cauchy problems, Eng. Anal. Bound. Elem. 35 (2011) 499–506.
[51] S. Rippa, An algorithm for selecting a good parameter c in radial basis function interpolation, Adv. Comput. Math. 11 (1999) 193–210.
[52] A.H.D. Cheng, M.A. Golberg, E.J. Kansa, Q. Zammito, Exponential convergence and H-c multiquadric collocation method for partial differential equations, Numer. Meth. Part. D. E. 19 (2003) 571–594.
[53] R.E. Carlson, T.A. Foley, The parameter $R2$ in multiquadric interpolation, Comput. Math. Appl. 21 (1991) 29–42.
[54] A.E. Tarwater, A parameter study of Hardy's multiquadric method for scattered data interpolation, Report UCRL-53670, Lawrence Livermore National Laboratory, 1985.
[55] G. Fasshauer, J. Zhang, On choosing "optimal" shape parameters for RBF approximation, Numer. Algorithms 45 (2007) 346–368.
[56] M.J.D. Powell, The Theory of Radial Basis Function Approximation in 1990, Clarendon, Oxford, 1992.
[57] M.D. Buhmann, Radial basis functions, Acta Numerica 9 (2000) 1–38.
[58] M.D. Buhmann, Radial Basis Functions: Theory and Implementations, Cambridge University Press, New York, 2004.
[59] H. Wendland, Scattered Data Approximation, Cambridge University Press, New York, 2005.
[60] M.A. Golberg, Some recent results and proposals for the use of radial basis functions in the BEM, Eng. Anal. Bound. Elem. 23 (1999) 285–296.
[61] G.N. Elnagar, M.A. Kazemi, Pseudospectral Legendre-based optimal computation of nonlinear constrained variational problems, J. Comput. Appl. Math. 88 (1997) 363–375.

[62] G.N. Elnagar, M. Razzaghi, A collocation-type method for linear quadratic optimal control problems, Optim. Control. Appl. Meth. 18 (1998) 227–235.
[63] J. Shen, T. Tang, High Order Numerical Methods and Algorithms, Chinese Science Press, 2005.
[64] G.N. Elnagar, M.A. Kazemi, M. Razzaghi, The Pseudospectral Legendre method for discretizing optimal control problems, IEEE Trans. Automat. Control 40 (1995) 1793–1796.
[65] W.W. Hager, Multiplier methods for nonlinear optimal control problems, SIAM J. Numer. Anal. 37 (1990) 1061–1080.
[66] E. Polak, T.H. Yang, D.Q. Mayne, A method of centers based on Barrier function methods for solving optimal control problems with continum state and control constraints, SIAM J. Optim. 31 (1993) 159–179.
[67] G.N. Elnagar, M.A. Kazemi, Pseudospectral Chebyshev optimal control of constrained nonlinear dynamical systems, Comput. Optim. Appl. 11 (1998) 195–217.
[68] G.N. Elnagar, M. Razzaghi, A collocation-type method for linear quadratic optimal control problems, Optim. Control. Appl. Meth. 18 (1997) 227–235.
[69] H.R. Marzban, M. Razzaghi, Optimal control of linear delay systems via hybrid of block-pulse and Legendre polynomials, J. Franklin Inst. 341 (2004) 279–293.
[70] F. Khellat, Optimal control of linear time-delayed systems by linear Legendre multiwavelets, J. Optim. Theory. Appl. 143 (2009) 107–121.
[71] M. Razzaghi, H.R. Marzban, Optimal control of singular systems via piecewise linear polynomial functions, Math. Meth. Appl. Sci. 25 (2002) 399–408.
[72] M. Razzaghi, Optimization of time delay systems by hybrid functions, Optim. Eng. 10 (2009) 363–376.